AIAA SPACE Forum
31 Aug-2 Sep 2015, Pasadena, California
AIAA SPACE 2015 Conference and Exposition

Flexible Electronics-Based Transformers for Extreme Environments

Marco B. Quadrelli[1], Adrian Stoica[2], Michel Ingham[3], Anubhav Thakur[4]
Jet Propulsion Laboratory, California Institute of Technology, 4800 Oak Grove Drive, Pasadena, CA 91109-

This paper provides a survey of the use of modular multifunctional systems, called Flexible Transformers, to facilitate the exploration of extreme and previously inaccessible environments. A novel dynamics and control model of a modular algorithm for assembly, folding, and unfolding of these innovative structural systems is also described, together with the control model and the simulation results.

I. Introduction

Extreme planetary environments represent the next frontier for in-situ robotic space exploration. Missions for exploration will be followed by robotic missions for exploitation, and by manned missions. All these missions have one common challenge: harsh, extreme environments (EE), where very low or high temperatures, high radiation, high pressure, corrosiveness, toxicity, and other factors make the missions inconceivable at present. We propose an enabling capability for operation in extreme environments, a solution applicable to all types of in-situ missions, which is to project and control a favorable micro-environment (around a rover) in the local area where exploration, exploitation or human visits will take place. The systems that could provide such a capability are, in the following, called 'Transformers', and were initially developed under a 2013 NASA Innovative Advanced Concepts (NIAC) Phase 1 task titled *Transformers for Extreme Environments*. The name suggests their two key properties: they transform the environment, and they adapt to needs by shape change/transformation. Their body surface would embed reflectors and solar cells; they would also include antenna elements for communication, and actuation and control elements for shape change. This novel concept has significant potential benefits for both robotic and human spaceflight. The multifunctional system concept discussed in this paper directly addresses the "Surviving Extreme Space Environments" Challenge, one of the NASA's Space Technology Grand Challenges[5], specifically aimed at enabling robotic operations and survival, in the most extreme environments of our solar system.

This paper investigates the feasibility and deployment of a novel technique based on flexible multifunctional deployable structures for modular and agile rovers to enable exploration of previously inaccessible terrain. The entire deployable is proposed to be built from a single, thin sheet, such a flexible substrate of Mylar, Steel or Plastics. This substrate would be manufactured as a thin (≈100 μm) and flexible layer, survivable to extreme environments, such as hot temperatures (Venus) or cold temperatures (Moon, Titan). Along its large surface, this entire sheet could be partitioned into modular 'Tiles' to serve different programmable purposes. This paper looks into the use of the flexible multifunctional systems for deploying large solar panels and also solar reflectors on the same plane so as to serve as a means of power generation and also directing the solar radiation onto a target body (e.g., a rover). The rover would find itself to be in a region not receiving sufficient solar radiation, hence alternative solutions to energy harvesting would be required. These multifunctional systems would allow for a tightly folded stowed configuration, which would self-unfold to take the shapes/functions needed by the mission targets, and then again transform their shapes as required.

The paper also systematically examines the system requirements in order to achieve this folding and unfolding actuation. The system level study also includes an analysis of the possible configurations for development of deployable multifunctional systems for this application, based on the current research and proven space technology.

---

[1] Corresponding author, Research Technologist, Robotics Controls and Estimation Group, Autonomous Systems Division, Mail Stop 198-219, AIAA Associate Fellow.
[2] Supervisor, Robotics Controls and Estimation Group
[3] Supervisor, System Architectures and Behaviors Group; AIAA Associate Fellow
[4] Graduate Student, Dept. of Mechanical Engineering, University of Southern California
[5] NASA Space Technology Grand Challenges, http://www.nasa.gov/pdf/503466main_space_tech_grand_challenges_12_02_10.pdf

After a preliminary analysis of the system level architecture, the paper describes the use of JPL's DSENDSEdu[6] modeling and simulation package for the control and dynamic modeling of articulated multibody systems. These deployable systems are currently being modeled as serially connected rigid bodies, which possess a repeating pattern. Exploiting this repetition and symmetry present in the structure, a function for mapping a symmetric pattern of five inter-connected bodies for any given square was developed and is further elaborated in the paper. This algorithm/function has been converted into a 'Tile Assembly', which incorporates feed-forward, and a Proportional Integral Derivative controller (PID) to actuate motors to obtain a desired configuration of the system. The PID controller calculates an "error" value as the difference between measured process variables and desired set points. This enables the system to minimize the deviation obtained during the deployment and folding process. Simulations were constructed to show the folding operations for larger deployed structures.

II. System Overview and Feasibility

Planetary exploration by means of autonomous rovers is limited by various factors primarily centered on the size and power generation capabilities of the rover itself. Installing a radioisotope thermoelectric generator (RTG) on a rover would enable it to sustain itself for the duration of the mission and thereby removing the dependence on solar energy. Due to the cost and complexity of the RTG, its mission design, mobility and maneuverability would be greatly compromised. As a result, a compact and agile design for the rover, required for exploration of intricate and scientifically valuable locations like caves and crevasses would be limited with an RTG. This section looks at the feasibility and deployment of a novel technique based on flexible electronic multifunctional systems (MFS) for modular and agile rovers to enable exploration of previously inaccessible terrain. The entire MFS is proposed to be built from a single, thin sheet; a flexible substrate of Mylar, Steel or Plastics (PEN, PI). This substrate would be manufactured as a thin (≈100 μm) and light flexible layer, survivable to extreme environments. Along its large surface, this entire sheet could be partitioned into modular 'Tiles' to serve different programmable purposes. This section looks into the use of the flexible MFSs for deploying large solar panels and also solar reflectors on the same plane so as to serve as a means of power generation and also directing the solar radiation onto a target body (ex. Rover) which is not receiving sufficient solar radiation. Flexible MFSs would allow for a tightly folded stowed configuration and it would self-unfold to take the shape/function needed by the mission target, and then again transform its shape as needed. This section systematically examines the system requirements in order to achieve this folding and unfolding actuation. The system level study also includes an analysis of the possible configurations for development of flexible electronics MFSs, based on the current research and proven space technology. We explore the use of flexible electronics as a basis for advancing the applications of space robotic exploration. Implementation of flexible electronic systems on rovers will provide improved mobility, modularity and maneuverability capabilities.

MFSs can be used in conjunction with rover exploration, projecting a favorable micro-environment into cold and dark areas. These applications are driven by the need for a thin, low mass, large area structure (e.g., polymer-based), which could not be implemented using conventional engineering materials such as metals and alloys. In each case, there is also the need to integrate sensing and control electronics within the structure. The following aspects of the system level design must be considered in order to establish the feasibility of this technology:

- Flexible Electronic Material:
  - Substrate
  - Backplane electronics
  - Front plane electronics
  - Encapsulation
- Actuators
  - Type
  - Size
  - Power
  - Control
  - Repeatability
- Packaging and deployment sequence

[6] http://dartslab.jpl.nasa.gov

- Thermal requirements

Figure 1 shows a simple outline of the components involved in the design of flexible electronics-based MFSs.

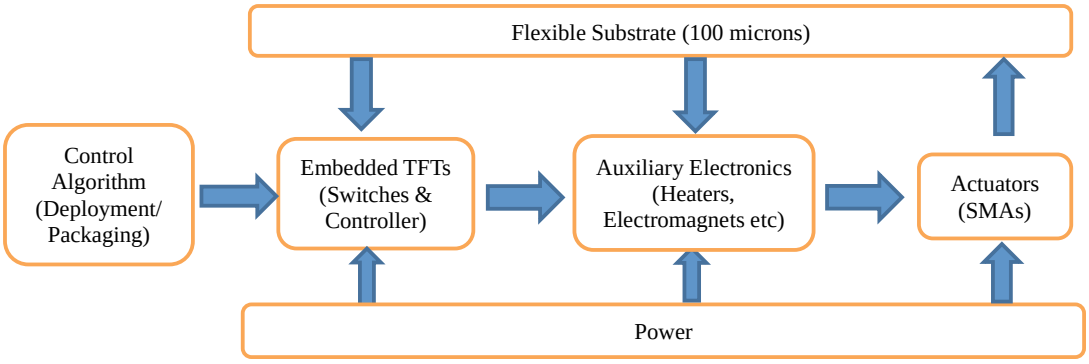

Figure 1. Simple outline of the components involved in the design of flexible electronics-based MFSs.

The flexible substrate on which the Thin Film Transistors (TFTs) would be embedded (or grown) and the actuators and auxiliary electronics mounted is the most crucial element. This would dictate the minimum bending/folding capabilities of the MFS without compromising the functionality of the embedded devices. The mounting scheme for the devices, which are to be externally mounted onto the substrate, would also influence the folding and deployment capabilities. The control algorithm would determine the crease pattern, which needs to be made on the surface of the substrate. This would also determine the actuation sequence for the actuators present on the substrate. The control algorithm would then be designed to minimize the number of overlapping folds and the number of actuators required to achieve complete deployment.

A. Options for thin layer fabrication

To provide the desired suite of functionality, the MFS surface may need to be quite large, and yet, if thin, it could be packed into a small volume during flight. Assuming the mission allows for a 1 m^3 packed MFS, a surface of ~100 microns, can unfold to an area of 10,000 m^2, i.e., a 100 m × 100 m square. Made of a gossamer-thin flexible multi-layer sheet, they may have one side covered with solar cells, and the other side with a highly reflective coating, while inner layers compute, self-actuate to change shape, store energy in batteries, and embed a spider-web antenna. All of these subsystem functions have been individually demonstrated on thin flexible layers of tens of microns thickness (some shown in Figure 2): power from solar arrays [1,2], avionics circuits [3], controls [4], sensing [5], shape-memory alloy actuation [6], communication circuits [7,8], and antennas [9]. The study will include system integration of the sub-systems by same-layer integration options, as demonstrated by Epidermal electronics [10] and by multi-layer stacking [11].

Figure 2. Sub-systems built on flexible layers: electronics, actuation, antenna, and solar cells; epidermal electronics (rightmost) integrate several of them in the same thin, peelable layer.

B. Options for fine-grain cellular architectures

The MFS fabric is likely to have a cellular structure, with each cell including multiple sub-system functions; cell communication is local. Distributed information processing, communications and control would be achieved by groups of cells. Both homogeneous (one cell type) and heterogenerous designs (multiple cells type with various primary sub-system roles), will be explored. The cells will have flexibility at their perimeter, forming a tessellated structure, which can change shape by actuation of elastomer joints at cell borders. Triggering the proper actuator groups in sequence produces a shape. This may follow an origami-type folding to form a diversity of 3D shapes. Work in these areas for specific sub-systems has been done under *programmable matter* [12] and *origami robots* projects [13]. An example of the use of origami in producing a large- scale foldable structure is the Eyeglass Telescope built by Los Alamos National Lab [14]. Some of these concepts are shown in Figure 3.

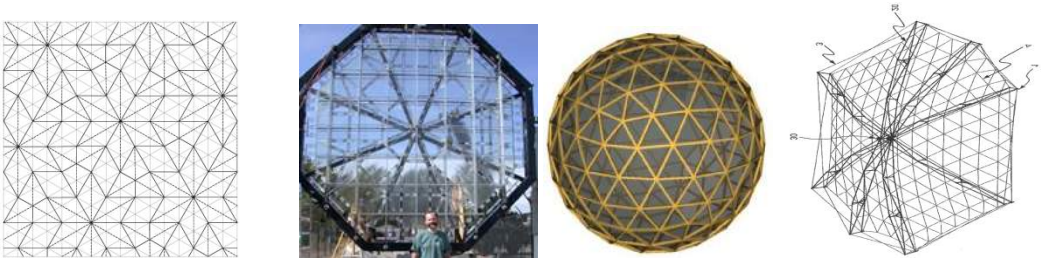

a) (b) (c) (d)

Figure 3. (a) Cellular architecture of T-fabric allows origami-like folding designs; (b) LANL Eyeglass telescope used origami-folding for a large structure (c) MFS as a sphere, (d) Japanese design for a deployable antenna [15].

III. Flexible Electronics-based MFS Design Configuration

Table 1 below shows two feasible configurations possible for flexible MFSs. An analysis of the reasoning behind the selection of these components/techniques is then made.

Property	Configuration 1	Configuration 2
Substrate	Steel	Mylar (PET)
Bending Radius	4cm	1.5 mm
Back Plane Electronics	a:Si-H (amorphous)	nc:Si-H (nano crystalline)
Actuators	Ni-Ti	Ni-Ti
Auxiliary Electronics	Heater coil, Electromagnets	Bidirectional SMA, Heater coil
Deployment technique	Box- Pleated folding config	Folding Cylinder

Table 1. Two feasible configurations for flexible MFSs.

Flexible Electronics Material Selection

Based on the application of this technology it is required that the material selected be bendable, rollable and elastically stretchable. The following equation is a good approximation for the strain developed in the material during bending: ε= d/2r, where, ε= strain, d= thickness, r= bending radius. Depending on the material selected, the strain limit can be decided. For example, for a Si:H (hydrogenated amorphous Si) sheet of 100 microns, strains of .1-1% can be tolerated without affecting the electrical performance of the device. In order to further improve the performance and bending characteristics of the device, the transistors are grown on the neutral plane to minimize the strain experienced by them during bending. A net-like configuration can be employed with the electronic transistors placed on the ribs of the net in order to improve the elastic characteristics of the device.

Substrate material requirements

The substrate requirements would be obtained as follows:

- T*g* (Glass Transition temp) must be compatible with the maximum fabrication temperature, i.e. $|\Delta CTE \times \Delta T| \leq (0.1\text{-}\ 0.3)\%$, where ΔT- Temp during extrusion, and ΔCTE- Difference in coefficient of thermal expansion.
- High thermal conductivity.
- High Young's modulus.
- Type (based on application):
  - Conductive substrate is usually preferred as it serves as a common node.
  - Insulating substrate minimizes the coupling capacitance.
  - Magnetic substrate is favorable in mounting applications.

The properties for substrates for flexible backplanes are listed in Table 2 [16]. Stainless steel possesses superior mechanical properties which favors its selection as a suitable substrate material. For the purpose of insulation it is required that the steel be covered by a layer of either SiN or SiO2. Mylar is also a possible choice for substrate material. Tellurium TFT has been shown to grow on Mylar, having a bending radius of 1.5mm [17]. Depending on the thermal requirements and the final mass constraint for the design, the choice of the substrate material can be made between Mylar, Steel and PI.

Property	Unit	Glass (1737)	Plastics (PEN, PI)	Stainless Steel 430
Thickness	microns	100	100	100
Weight	g/m^2	250	120	800
CTE	Ppm/deg C	4	16	10
Elastic Modulus	GPa	70	5	500
Max Process Temp	Deg C	600	180,300	1000
Safe bending radius	cm	40	4	4

Table 2. Some properties for substrates for flexible backplanes

Backplane Electronics

In regards to backplane electronics, although many promising results have been reported with organic semiconductors, the performance and lifetime of such devices suffer from low carrier mobility and poor chemical stability, which hinders their use for most electronic applications. On the other hand, inorganic semiconductors provide superior carrier mobility and chemical stability. However, the great challenge lies in integrating brittle inorganic semiconductors on flexible substrates while preserving the structural and electrical properties. Transfer-and-bond approach and Direct fabrication methods are two available approaches to bond the inorganic TFTs to the substrates listed earlier. Direct fabrication method relies on polycrystalline or amorphous semiconductors because these can be grown on foreign substrates. The requirements for backplane electronics material are:

- Rugged
- Rollable
- Bendable
- Capable of CMOS operation

Examples are:

- Silicon TFT: These materials benefit from well-established technology for manufacturing and processing.
- Hydrogenated Amorphous Si TFT (a-Si:H), Substrate Temp: 250-350^{o} C, Used for developing n-channel MOSFET, Developing technique: PECVD
- Nanocrystalline Silicon (nc-Si:H), Substrate Temp: 250-350^{0} C, CMOS capabilities, Developing technique: PECVD.

Interconnects and Contacts

The critical crack strain for the connectors is inversely proportional to the square root of the substrate thickness. To develop stretchable and bendable interconnects the following techniques were adopted: 1) Combining Elastomers with conductive polymers; 2) Combining Elastomers with metal particles; and 3) Metal film encased in elastomers. Studies conducted by Wagner et al [18] have shown that compressive stress in the gold film induces spontaneous wrinkling, which can shrink the net length of the thin-film conductors by several tenths of a percent, intending to make use of this strain to raise the stretchability of the gold films above their fracture strain of, typically, 1%. Thin metal films—typically, 100-nm-thick layer of gold on top of a 5-nm-thick adhesion interlayer of chromium— were deposited in one run by successive electron beam evaporation onto elastomeric substrates of PDMS held at room temperature. It was experimentally discovered that the stripes can retain electrical continuity when stretched by as much as 22%.

Actuators

The selection of the actuators is dictated by the following constraints:

- Power requirement for deploying and folding
- Displacement achieved
- Actuation force (torque)
- Size
- Compatible with TFTs

Based on the constraints listed above, the following actuators have been considered:

- Electroactive Polymers (EAP):
    - Principle: The EAP actuator can be modeled as a capacitance with compliant electrodes, where the insulator is the dielectric polymer, as shown in Figure 4 [19]. When an electric field is applied across the polymer, an electrostatic pressure, also known as the Maxwell stress, rises between the charged electrodes bringing them closer together, and spreading them out. Due to this the film expands sideways when squeezed in thickness.
    - Power Requirements: EAP can undergo large actuation strains of up to 200% under electrical stimulation of typically 100-150 V/m.
    - Drawbacks: Actuation Type: Linear- A lever arm mechanism or coupling would need to be developed to achieve folding of the flexible substrates. Displacement: ~ 30-45 microns. EAP is compatible but not ideally suited for this application.
- Actuator Based on Polypyrrole:
    - Principle: The conjugated polymer polypyrrole undergoes a volume change of several percent when its oxidation state is changed electrochemically. Illustration shown in figure 5 [20].
    - Actuation Displacement: 0-180^{0}. Actuation Voltage: 0 to -1V. Energy: Mass ratio – 40mJ/g. Power Density: ~7.5mW/g.
    - Drawbacks: The polymer must be in contact with an electrolyte that can serve as a source/sink of ions in order for this reaction to occur; since an aqueous solution of NaDBS is used as an electrolyte, this design would not be suitable for space use.
- Actuators based on Shape Memory Alloy: The most common SMA is Ni–Ti (Nitinol) alloy, used for its ductility, and fatigue and corrosion resistance.
    - Principle: Heating past the alloy's transition temperature results in a change in the crystal structure, in which the martensite composition of the alloy turns into austenite crystals. This shift is called 'twinning' and a shape change is associated with this twinning. In order to concentrate the heating near the axis of rotation a heating coil (Ni-Cr coil) is employed. As the actuator is no longer part of the circuit, only two ends need to be fixed to the substrate at opposite sides of the

actuated joint. The elimination of electrodes simplifies the shape and enables further miniaturization. On the basis of the tests conducted by Paik et al [21], the values for the actuators are listed below.

- Actuation type: Torsional actuation (0-180^{o}). Dimensions: 12mmx 7mm x100 microns (thickness). Minimum Bend radius: 500 microns. Power Requirements: 180^{0} actuation - .19A at 13V (Heating coil). Power Consumption: 3.6W. Mass: 68x 10^(-6) Kg. Torque: 0.0045Nm.
- Drawbacks: The SMA tends to fatigue at 5% strain after 100 cycles.
- Given the size of the actuator and the range of motion it provides, Ni-Ti based SMA can be considered to be a preferred choice for actuator for the purpose of deploying and folding of flexible electronics based MFSs. Two SMA actuators can be used with their rotation aligned opposite to each other to obtain a bi-directional actuation.

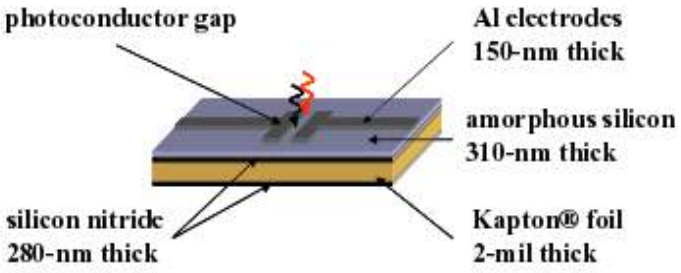

Figure 4. The EAP actuator can be modeled as a capacitance with compliant electrodes, where the insulator is the dielectric polymer [19].

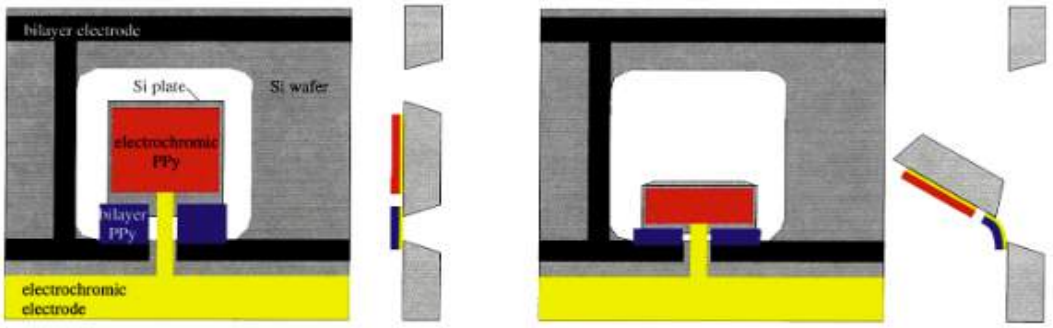

Figure 5. Actuator Based on Polypyrrole [20].

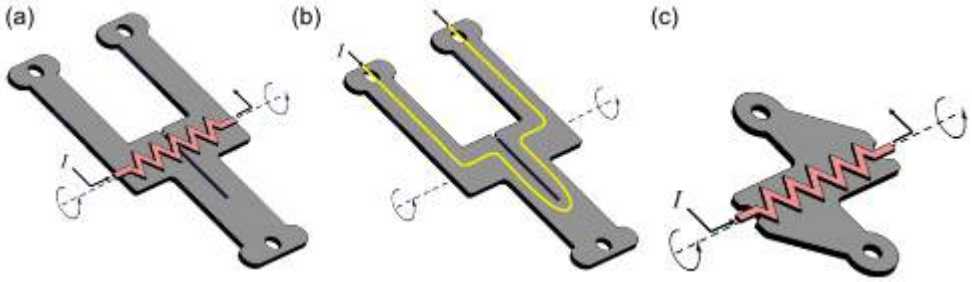

Figure 6. Actuators based on shape-memory alloy [21].

Different configurations were examined to determine the most reliable, modular and cost effective solution possible for the deployment of flexible electronics based MFSs on rovers for the purpose of exploration of extreme and previously inaccessible terrain which was deemed untraversable due to size and power constraints.

Table 3 illustrates the possible configurations of substrate material, backplane plane electronics, actuators, and folding and unpacking techniques based of existing technology and on-going research capable of executing the task of deploying and controlling a flexible MFS. The table is ranked in order of preference. The rank is assigned based on the feasibility, reduction in area achieved, complexity and cost.

Mylar is selected as the primary choice for the flexible substrate material due to its inherent thermal insulation capability and its ability to withstand extreme temperature variations. Tellurium is show to be grown on a 100μm thick layer of Mylar. Tellurium can be used to fabricate CMOS components on Mylar, which allows for controller design within the substrate layer itself. The use of Shape Memory Alloys (SMAs) would be the most efficient means for achieving actuation for the flexible MFS given the power and mass constraints. Solenoid coils can be printed on the substrate layer, which once activated would allow the folded substrates to be held together by means of the magnetic field generated by the solenoids. Solenoids can be replaced with embedded electromagnets, which would facilitate stronger attraction/ repulsion forces between the folds but would also impose a higher power and mass requirement.

Rank	Substrate	Back Plane Electronics	Actuators	Bending Radius	Folding and Deployment	Comments
1.	Mylar	Tellurium	SMA & Printed solenoids	1.5mm	Folding Cylinder (Fig. 13)	Folding system pending analysis
2.	Steel	nc-Si:H	SMA & Electromagnets	40mm	Box- Pleated (Fig. 5)	“
3.	Plastics (PEN, PI)	nc-Si:H	Two SMA: With opposing folding axes	40mm	Box- Pleated (Fig. 5)	“
4.	Glass	a-Si-H	Polypyrrole based actuator (Fig. 3)	400mm	Rolling	“
5.	Steel/Mylar	a-Si:H/ nc-Si:H	Spring Hinges/ Motors	Discontinuous: Not a single sheet	Solar Array	Flight tested
6.	Mylar/ Steel/ Plastics	a-Si:H/ nc-Si:H	Spring Hinges/ motors	1.5mm to 40mm	Parabolic Reflectors	Flight tested
7.	Mylar/ Steel/ Plastics	a-Si:H/ nc-Si:H	Compressed Air	1.5mm to 40mm	Inflatable antennas	Flight tested

Table 3. Possible configurations of substrate material, backplane plane electronics, actuators, and folding and unpacking techniques based of existing technology and on-going research capable of executing the task of deploying and controlling a flexible MFS.

IV. Folding and Deployment Techniques

For the deployment of flexible MFS, it is critical to estimate the most efficient pattern of creases on the surface of the plane which needs to be folded. The pattern of the crease selected and the order in which the substrate is folded will be discussed further in this section. On the basis of the research conducted by Demanie et al [22] it was shown that a n x n box pleated crease pattern is capable of reaching any folded state without the material penetrating itself. Figure 7 shows an 8x8 box pleated crease pattern. This pattern can be considered suitable for our application since it provides the capability is varying the final deployed configuration of the MFS (reflector) and modifying it as the environment may dictate.

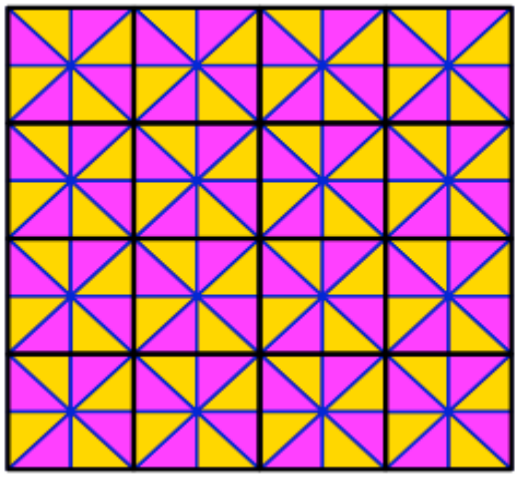

Figure 7. An 8x8 box pleated crease pattern.

In order to achieve a fold along the crease, actuators are required to be placed at the diagonals and the edges of the squares as shown in Figure 8 for a 4x4 box pleated crease pattern. Similar experiments have been conducted at the Distributed Robotics Laboratory at MIT to explore the capabilities of folding systems [23].

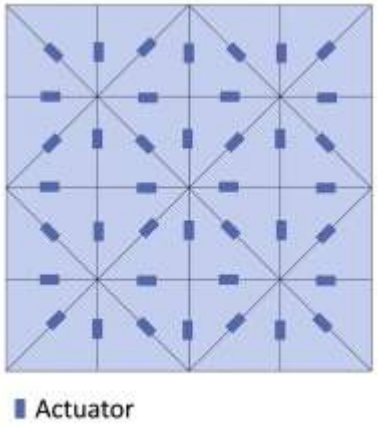

Figure 8. An actuated 4x4 box pleated crease pattern.

The smallest folded configuration formed from the pattern shown above would have a surface area equal to the area of the isosceles triangle into which the square has been divided. The strains in the folded state would be comparatively high and are required to be examined in detail to judge the feasibility of the folded state.

The folding algorithm design would depend on the final folded configuration of the plane, and would aim to minimize the strain levels in the creases and minimize the number of actuators to be used.

A representative pattern for a 4x4 plane folding into a unit isosceles triangle is shown in Figure 9.

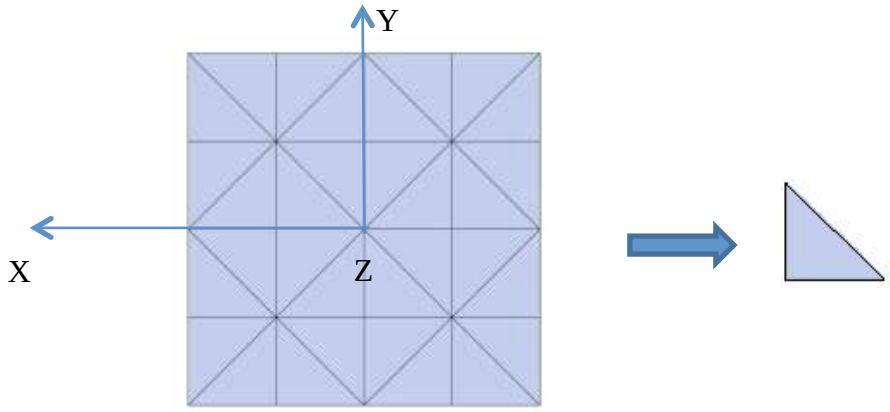

Figure 9. Folding to an isosceles triangle.

In order to keep a fixed coordinate reference for the plane, the folding operation is performed symmetrically about the Z-axis (into the paper) passing through the center of the plane. The reduction in area obtained for a 4x4 box pleated design is 96.7%. This is done ignoring the minimum bending radius to be considered for the substrate and the devices mounted on it. We also assume that the creases fold perfectly to 180^{o}, which would not be the case in the actual scenario. The folding is done sequentially, that is, the 4x4 matrix is first reduced to a 2x2 which is then finally folded into an isosceles triangle. The steps involved in the folding operation are described below with the help of Figure 10.

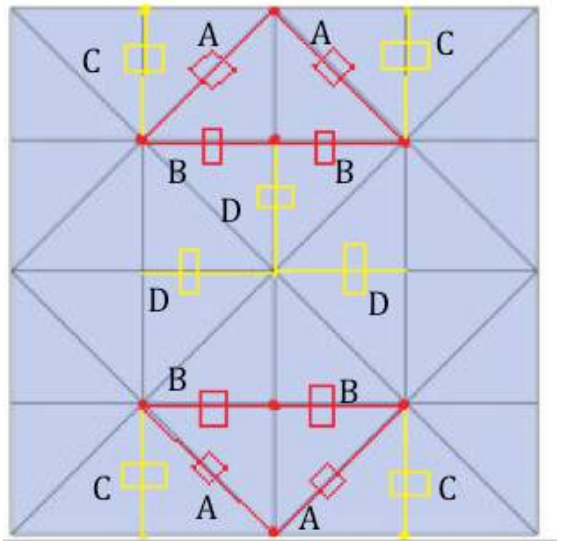

Figure 10. Sequence of folding operations to obtain triangle.

The red and yellow creases indicated folds in opposite directions to each other. The number of actuators required is 15, and the number of folds is 10. Actuating the SMA actuators A and B results into the formation of 2x2 box-pleated plane. Actuators C and D will finally result in the formation of a unit isosceles triangle.

V. Deployment and Packaging Mechanisms

A power efficient and realizable method for deployment of the flexible electronics based reflector/array is necessary. We have shortlisted SMAs as a possible means of achieving the maximum actuation in the most power

efficient manner. Incorporating the use of SMAs with electromagnets results in an efficient deployment and packaging technique. This technique involves the use of 1 electromagnet in combination with 1 (or 2 for better efficiency) SMA actuator(s). Figure 11 shows a flexible electronic substrate with incorporated SMAs and electromagnets fabricated at the Distributed Robotics Laboratory at MIT [24].

Figure 11. Flexible electronic substrate with incorporated SMAs and electromagnets fabricated at the Distributed Robotics Laboratory at MIT [24].

In Figure 11, the magnets are used to hold the flexible MFS in the stowed configuration. The polarity of the magnets is reversed to allow the MFS to deploy. The stiffness of the SMA at the creases helps with achieving a fully deployed state. The use of 2 SMAs with their axes of rotation opposite to each other can improve the mechanical efficiency of the system and also provide a shorter deployment time. Apart from embedding the electromagnets into the substrate, the solenoid coils can be printed on the flexible electric substrate and used to hold or deploy the MFS. This method insures the weight of the flexible MFS is kept to a minimum. In order to stow the MFS, the SMA is actuated in a predefined sequence which starts to fold the plane along the creases in order to go back to the stowed configuration. Once the plane folds along the creases, it is held together by means of magnets present on the 2 folded halves. This reduces the duty cycle of the SMA actuator considerably and improves the overall power efficiency.

Apart from the folding technique discussed above, there are numerous other ways to achieve a compact folded structure. The design to be selected will also need to be integrated with the rigid structural components and mechanism accompanying the flexible MFSs for the purpose of stability and mobility (rotation of the reflector). These methods include tailoring existing technology, which has been proven reliable in similar domains to fit the requirements for use in the application of flexible MFSs. These systems may include solar panel array deployment and deployable parabolic reflector antenna systems. For example, large parabolic reflectors have been deployed in space successfully and can provide a strong foundation for establishing similar deployment techniques for flexible electronics based MFSs.

Figure 12 shows an image of a deployable multiple-element antenna (MEA) antenna [25]. The surface area reduction is much less and the requirement for mechanical / structural support systems is much higher in comparison to the technique described above. This influences the final mass and the MFS's ability to pack compactly into a small volume.

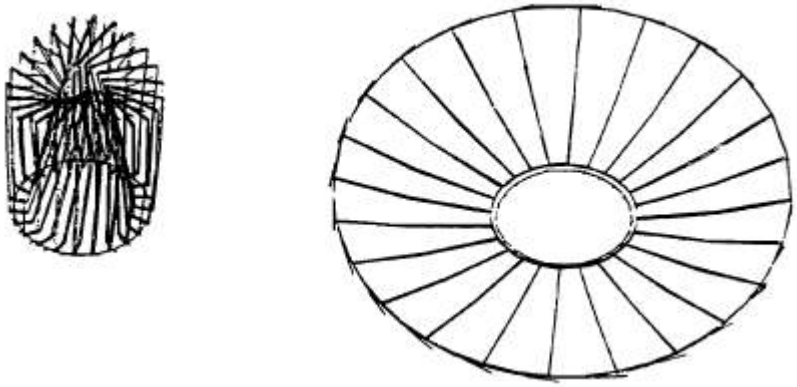

Figure 12. Deployable MEA antenna [25].

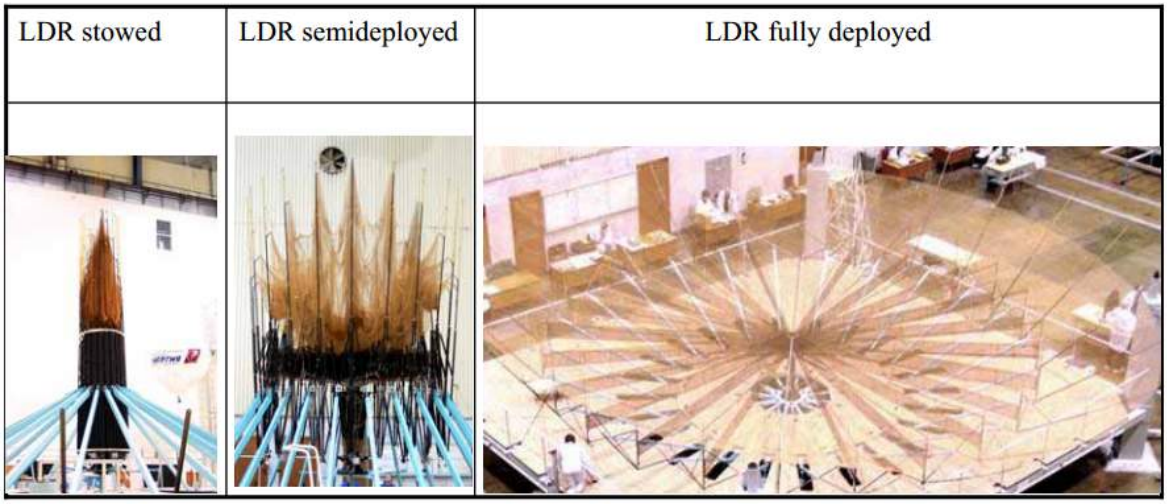

Figure 13. ESA Deployable Antenna [26].

The antenna shown in Figure 11 has been developed by the European Space Agency to provide global coverage in applications relating to Earth observations and science applications. The specifications for the antenna are obtained for the ESA LDA design section [26]. The deployed diameter was 12m and the total mass was 70kg. The advantages are that the number of folds is reduced considerably. The external skeleton structure simplifies the folding sequence, which can potentially reduce the strain developed in the flexible MFS. The reduction in strain can improve the fatigue life. There are also drawbacks. The current design is a one-time deployment and does not allow the antenna to be repackaged once it has been deployed. This means that a refolding mechanism needs to be added to the device in order to satisfy all requirements for the purpose of flexible MFSs for extreme environments. Due to a heavy reliance on the external skeleton structure, the mass of the overall system is high.

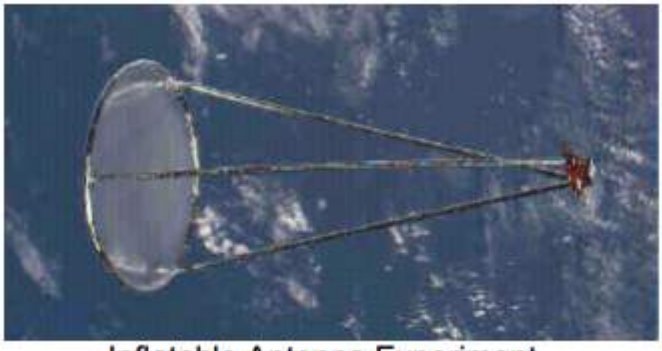

Figure 14. Inflatable Antenna Experiment [27].

Inflatable deployment techniques possess capabilities which can more easily be incorporated into deployment of flexible MFSs in comparison to rigid antenna deployment systems as discussed earlier. By eliminating the need for an exo-skeleton structure to achieve the fully deployed configuration, the overall mass, size and the ability of the system to pack compactly is significantly reduced. Figure 14 shows the IAE satellite with the fully deployed reflector antenna [27]. The advantages are that no requirement of rigid structure which results in reduction in system mass and stowed volume. Proven technology which can be tailored to meets the needs of flexible electronic MFSs. The drawbacks are the one-time deployment: once the existing system is deployed, it stays in the fully

deployed state. A new mechanism would have to be introduced to deflate the inflated structure. The air would have to be stored in tanks available on-board. Depending on the size of the MFS, the size of the tanks would be determined. This would add to the overall volume requirements for the system. Loss in air pressure can be a single point of failure and can also induce instability into the system.

Flexible Electronics Based Folding Cylinder Deployment Technique

This technique is being analyzed solely for the purpose of achieving an efficient deployment for a flexible electronic based MFS for extreme environments. This technique tries to incorporate existing technology described above with novel features of flexible electronics embedded with SMA actuators in order to achieve an efficient deployment and folding scheme utilizing the minimum resources. Even though the reduction in area achieved between the stowed configuration and the fully deployed state is not as high as discussed in the box-pleated folding technique, the number of folds and the angles at which the plane is folded induce a considerably lower amount of strain on the flexible MFS, thereby reducing the amount of fatigue it will undergo. The folding cylinder technique eliminates the need of compressed air tanks and minimally relies on an external structural support system for deployment and folding as in the case of inflatable antennas and large deployable antennas respectively. Figure 15 shows the steps involved in achieving a fully deployed state from a flexible electronics-based folded cylinder MFS [25].

The flexible substrate embedded with SMA actuators is rolled into a cylinder. This can be achieved by means of utilizing the SMAs present on the substrate itself or by means of an external mechanism. The number of rolls about the center axis will determine the radius of the cylinder. It needs to be noted that while rolling the plane into a cylinder, the creases must align if the rolls overlap, thereby forming multiple layers. Performing this rolling task will result in achieving the configuration as shown in figure 15B. Once the cylinder is obtained, the compression operation can begin in order to obtain the final stowed configuration of the MFS as shown in figure 15C. This technique relies on the minimal use of externally mounted structures and compressed air tanks. With respect to a single crease, the folds are not additive. That is, the number of overlapping folds is minimized. The strain produced on the substrate can be controlled by adjusting the diameter of the folding cylinder obtained by rolling the flexible electronic substrate. In order for the compression operation to work efficiently the creases in the different layers must align with the corresponding crease in the subsequent layers. This would require a higher amount of precision by the SMA actuators.

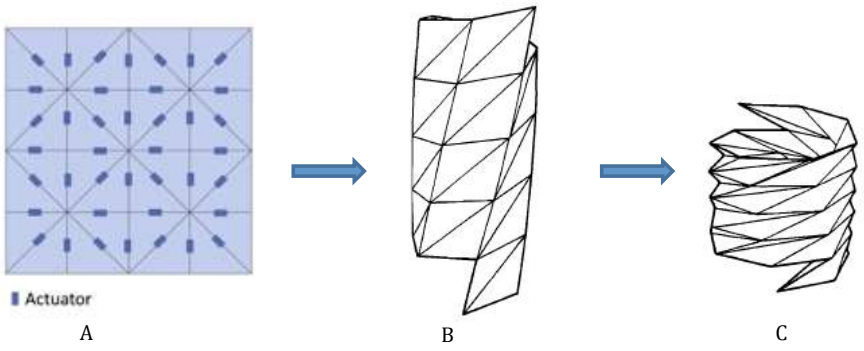

Figure 15. Steps involved in achieving a fully deployed state from a flexible electronics based folded cylinder MFS [25].

VI. Dynamics and Control of Representative Transformer Element

In order to better understand the behavior and folding operation of serially connected rigid bodies consisting of upwards of more than 200 elements, a dynamics model for the full system was developed. The torque requirements

for these Transformers were examined and have been elaborated in the sections below. Various control techniques were examined to determine the most efficient deployment and folding methodology. This paper describes the results for the following two simulations:

- Serial Link Assembly with Feed Forward Control;
- Level 3 Transformer Folding and Deployment Operation.

Transformer Design

The Transformer design is based on a serial chain model. The presence of closed chains is avoided for the purpose of reducing the complexity in the dynamic analysis and thereby targeting more accurate and replicable results from the simulations. The distinction between closed chain systems opposed to a serial chain, is that the end effector or the last linkage is connected to its base by means of a joint. This implies that in order for the model to produce a valid solution, these linkages forming a closed chain must act together. As an advantage a closed chain system provides additional rigidity for the same overall mass as a serial chain design.

Figure 16 shows a unit cell model of the transformer, which is its elemental building block. This design would be repeated multiple times in order to obtain the desired size of the transformer. The metric for establishing the size will be mission dependent and is not within the scope of this paper.

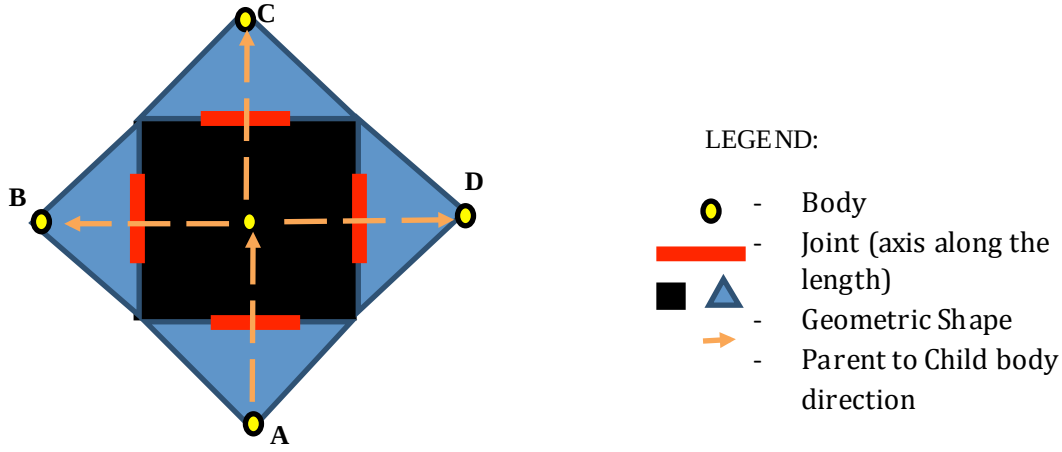

Total Number of Bodies- 5
Number of Joints - 4

Figure 16: Elemental Building Block

Each unit cell consists of five bodies, represented above by yellow circles. Bodies B, C and D are child bodies of center body O, which in turn is the child body of A. The cell consists of 4 PIN joints represented by red rectangles with the axis of rotation along its length. The resolution of the final folded configuration will be dependent on the size of the black center square.

Dynamics and Control Model

Simulation of Serial Link Assembly with Feed Forward Control

The terminology defined in this section will be carried forward through the reminder of the paper and is consistent with the simulation developed using the DSENDSEdu software package [28].

The serial chain represents a multi-body system having interconnected rigid bodies. Every rigid body in the chain has only one parent and one child body, except for the base body; which has no parent and the tip body which has no child. This arrangement of bodies is illustrated in Figure 17 [29] in the system overview section below. The rigid bodies, or links, are constrained by their connections to other links.

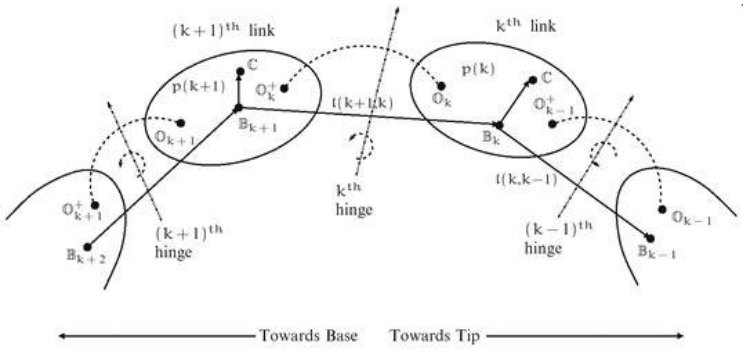

Figure 17: Links in a Serial Chain system [29]

The terminology used for defining the topology of the overall chain and the individual joints and frames associated with the rigid bodies is obtained from [29] which carries forward to the DSENDSEdu simulation software. This ensures consistency amongst the analytical and programming approaches being implemented.

The neighboring links in the direction towards the base (tip) is referred to as the inboard (outboard) link. The serial-chain is assumed to have a total of n links (and thus, has n hinges). Without loss in generality, the links are assumed to be numbered from 1 through n from the tip to the base.1 The k^{th} hinge connects the $(k+1)^{th}$ and the k^{th} link, as illustrated in Figure 1. Frames: O^k and O_k^+, attached to the k^{th} and $(k+1)^{th}$ links.

Simulating Level Three Folding and Deployment Operation

The configuration of the unit cell is defined by specifying the in-board body and the body to joint distances between the parent and the child bodies. Each of the joints of the unit cell is associated with a profiler, encoder and a PID controlled motor assembly.

The profiler is used to specify the rotation of each joint. In this case the rotation at each joint is specified as 3.14 radians. The encoder provides the measured value of the angle at every instant; this is then used to compute an error (measured – desired angle) which is fed into the PID controller. The folding operation being represented by PID motors will be carried out by Shape Memory Alloys (SMAs) in the final design.

The sequence of operation which governs the order in which the folds will occur is specified by implementing a Finite State Machine (FSM) in the simulation. The FSM controls the order of folding operations by specifying the time after which the next operation needs to be executed.

An increase in "level" increases the number of bodies and joints present in the Transformer. This increase can be represented by the following expression:

$$No.of\ Bodies = 4^n + 1$$
$$No.of\ Joints = 4^n$$

where n represents the level at which the bodies and joint to be calculated are present.

In this paper we discuss the design and dynamically modeling of a level 3 topology Transformer. This translates into a Transformer consisting of 65 rigid bodies and 64 pin joint. Implementing this system manually would be an extremely elaborate process. For this purpose an algorithm was developed to auto-generate and map the bodies and associated joints in the required topological order given the level (or depth) of the Transformer being designed. This

algorithm will not only reduce the complexity of the code but also facilitate ease in manipulating and modifying the configuration.

The level 3 configuration involves the unit cell configuration described above connected orthogonally to each other at one of the free corners, as depicted in Figure 18.

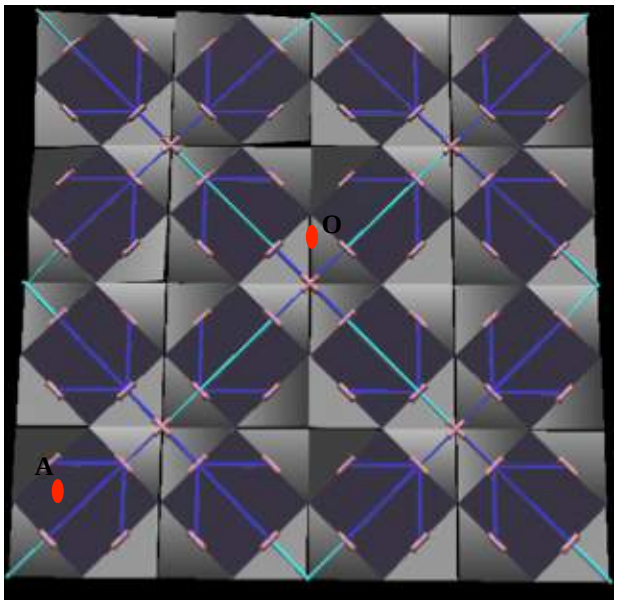

Figure 18: Level 3 Full Deployed Config –Tile Assembly Level 3

As shown above, point 'O' depicts the axis of symmetry at which the individual unit cells are attached. To propagate to the next level, the point of symmetry will be shifted from 'O' to 'A' (Bottom left corner). Now, three additional sets of level two configurations would be rotated and attached to A to form a level 3 configuration. This algorithm is described in a later section and is utilized to generate the topology of bodies and joints at a particular level.

Tiling Algorithm – for Constructing and Connecting Tiles in a Pattern

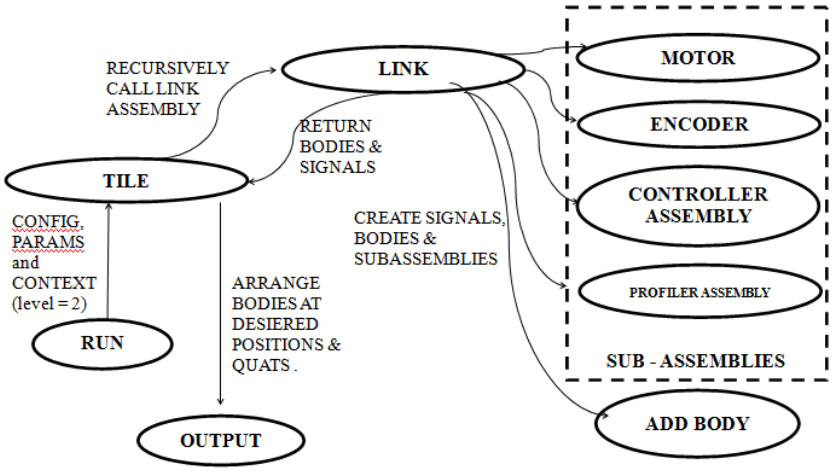

Figure 19: Tile Assembly Architecture

The block diagram illustrating the overall architecture for Tile Assembly is shown in Figure 19. The block diagram depicts the interaction of the parent assembly, Tile Assembly, with its child assemblies and subassemblies, Link/SubLink Assembly.

The run script provides the assembly with the required parameters like the mass properties for the bodies, their geometries and the level of the final pattern desired ('n' level). The algorithm for creating and attaching the bodies in the desired pattern is derived from the 'makeTile' function call described in the earlier report. The difference being that in this case instead of recursive calls creating the DARTS bodies and attaching them, Tile Assembly recursively calls Link Assembly at every level.

Link Assembly, which is an existing Dshell Assembly, is responsible for creating the bodies. It also has the following subassemblies associated with it.

- Motor Assembly- attaches a motor via a pin joint to the body created.
- Encoder Assembly- provides the actual position (angle) of the motor, its velocity and rates to the controller.
- Controller Assembly- Sets up the PID controller to operate the motion of the hinge associated with the body.
- Prolife Assembly- Generates an input function for the motor based on the desired angular displacement, velocity and rates required by the user.

Each call of Link Assembly returns a body connected to a motor by a hinge joint. The motion of this joint is defined by the profiler and the actual angles and rates can be obtained as flow outs from the encoder associated with the joint. Controller sets the gains for the system and ensures optimum operation. A feedforward signal can also be provided to the controller to improve the overall performance of the system. The Tile Assembly would recursively call Link Assembly depending on the level defined in the configuration dictionary of the run script. As a result all assemblies returned by Link Assembly would have bodies, motors, controller and profilers associated with them. The Tile Assembly is responsible for taking the assemblies returned by Link Assemblies and arranging them in the desired pattern. The pattern is alterable and can be defined by setting the in-board body to joint distance and the in-board body to joint quaternion.

Transformer Actuation Sequence

The prescribed actuation of the joints of the MFS from the initial state to the final state is depicted in figure 20 below.

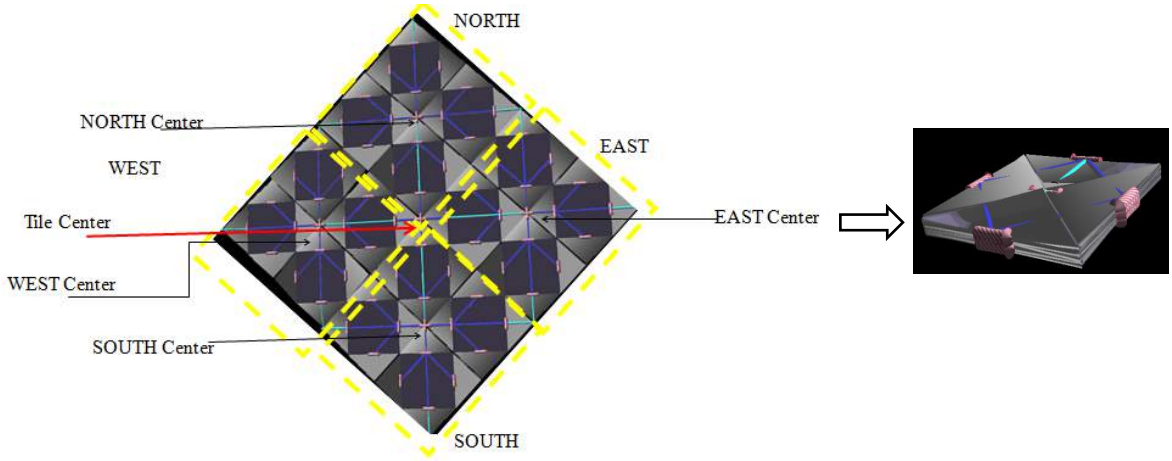

Figure 20: Transformer Quadrants

-

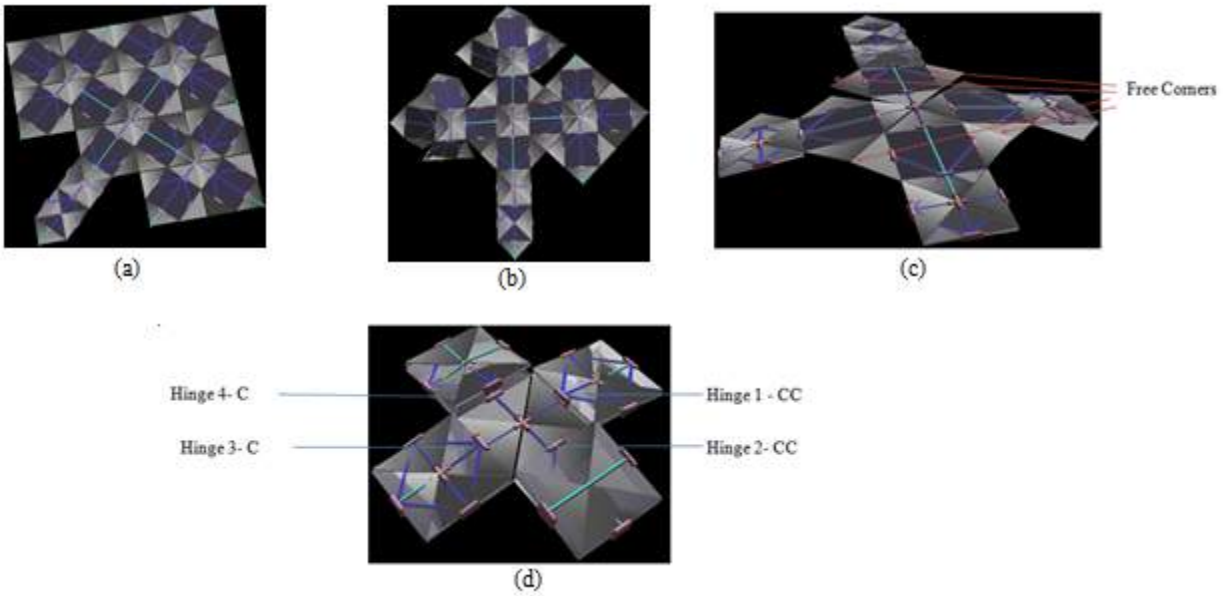

Figure 21: (a) 'Bar' configuration (b) North and West Quadrant Actuation (c) East Quadrant Actuation (d) 'X' configuration

Numerical Results and Discussion

Simulation Results for Level 3 Transformer Folding

Due to symmetry about the Tile center as depicted in Figure 20, the joint torques and center of mass (CM) displacements are examined only for the North quadrant. The torque requirement for the remaining three quadrants would be identical to the results obtained from the North quadrant.

It can be observed from the simulation that after every folding operation the torque requirement for every subsequent fold increases. This is because the joints closer to the Tile center have to displace a mass equal to the sum of all masses of the individual segments connected to that joint and present on the out-board direction. Based on the maximum value of torques obtained for different scenarios, the actuators would be accordingly selected.

The actuation of the joints was obtained by providing an input to the profiler, which then operates the motor, encoder and PID systems.

Profiler Input: Angle of rotation to Joints.
Outputs-

- Center of Mass Displacement vs Time for each individual links (Figure 22).
- Torque outputs for motors being actuated in the serial chain (Figure 23).

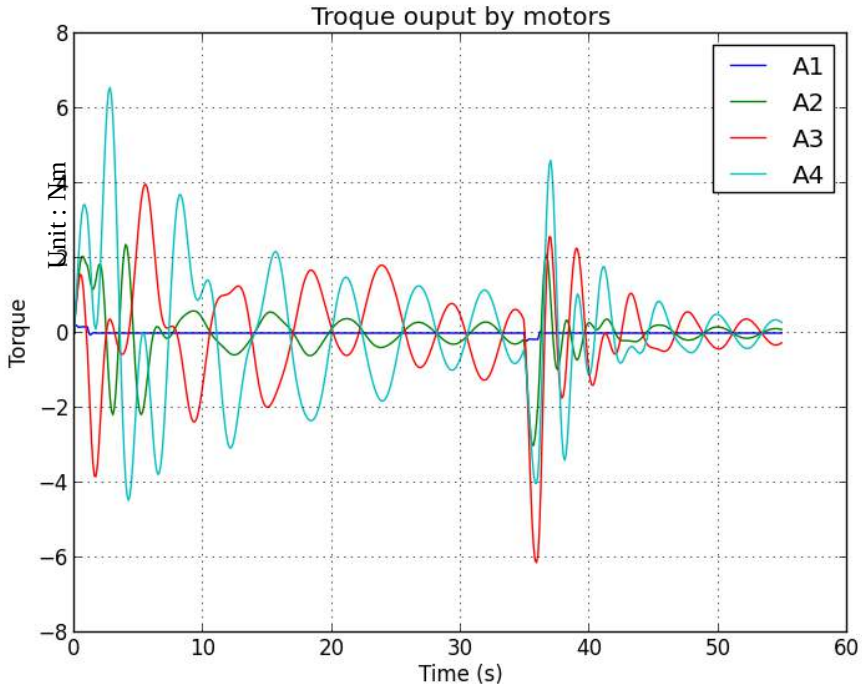

Figure 22: Torque Output for Motors (North) VS Time

The torque vs time characteristics shown in figure 45 allow for approximations on the minimum torque output required from the shape memory alloys (represented by PID motors in the simulations) to achieve a fully deployed/ folded configuration. The peaks shown in Figure 45 indicate the maximum torque values which would be exerted on the Transformers during the deployment and folding operations due to the actuation of the SMAs present at the joints.
It can be seen in Figure 22 that as the joints move closer to the Tile center, the torques required to actuate the joints increase.

- A1: Free Corner (Outer most)- Body Name: TileN_N_1_1__N_N_N. Maximum Torque = 0.268 Nm.
- A2: Center body for outer most link. Body Name: CentralLink_1_1__N_S_N. Maximum Torque= 3.130 Nm.
- A3: Body Name: TileW_N_1_1__N_N_N. Maximum Torque= 7.963 Nm.
- A4: Hinge 2 CC (fig 9- Final fold). Body Name CentralLink_1_1__N_W_N. Maximum Torque= 13.852 Nm.

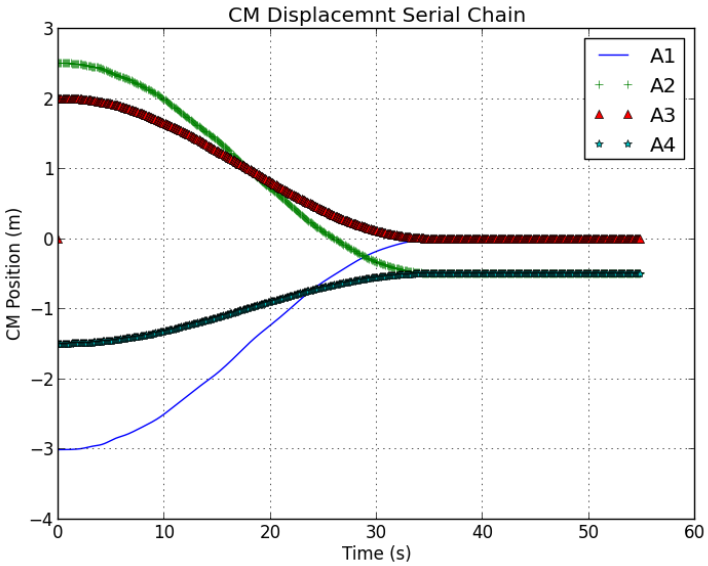

Figure 23: CM Displacement Level 3 Folding

The graph in Figure 23 shows the motion of the center of mass of the individual segments of the level three Transformer configuration. For the purpose of simplicity only 4 of the 256 CM displacements are shown in the graph. A3 and A4 folds in the direction opposite (counter-clockwise) to the other segments and hence has a peak displacement in the opposite direction. The slope of the peaks shown in the graph above can be adjusted by changing the maximum velocity and acceleration inputs provided to the profiler.

VII. Conclusions

This paper has surveyed the use of modular multifunctional systems to facilitate the exploration of extreme and previously inaccessible environments. After studying the current available technology and the on-going research it has been determined that the 2D solution (flexible substrate) is easier/cheaper to fabricate, packs more compactly, and ensures a wider range of capabilities as compared to the current techniques being employed like RTGs, deployable antennae and solar panel structures. Mylar-based substrate material with Tellurium back plane electronics are considered one of the leading prospects for flexible electronics due to its small bending radius and high thermal insulation capabilities. The use of Shape Memory Alloys (SMAs) has been determined to be the most efficient and reliable mean of actuation and control of the flexible MFS. Folding and deployment techniques like the box-pleated and the folding cylinder have also been considered. For an accurate trade-off between these techniques, a dynamic multi-body model for folding the tiles should be investigated in detail to determine the total work needed to achieve a fully packed state from a fully deployed one. The amount of strain generated due the folding operation in each of these methods would be an important metric to consider in determining the most efficient folding and deployment technique for the Transformer. The paper has also described the development of simulation models to enable the deployment and folding of a cellular system, by means of active feedback control. The model includes an algorithmic treatment of the multiple levels of tiling, and the active control that enables this complex structure to be folded/unfolded in any arbitrary topology.

VIII. Acknowledgements

This research was carried out at the Jet Propulsion Laboratory, California Institute of Technology, under a contract with the National Aeronautic and Space Administration. The authors are grateful to Dr. Abhinandan Jain of JPL, for his insight and help in guiding Mr. Thakur's simulation work using the DARTSLab simulation framework (http://www.dartslab.jpl.nasa.gov)

References

[1] Sasaki,T Suzuki,H, "Real-Time Structural Analysis of Compositionally Graded InGaAs/GaAs(0 0 1) Layers" IEEE J Photovoltaics 2012, V2, 35

[2] Lo et al: Fabrication of Flexible Amorphous-Si Thin-Film Solar Cells on a Parylene Template Using a Direct Separation Process , IEEE Trans. Electron Devices 2011, V58, pp. 1433-1439.

[3] Meichun Ruan, "Latching micromagnetic relays" IEEE Conf MEMS 2001, 511

[4] Jun Cao, Xinmin Lai, "A systematic method of adaptive joint design considering different assembly sequence in sheet metal product," The International Journal of Advanced Manufacturing Technology, v34, Sept. 2007

[5] Jiang, F., Tai, Y-C, Walsh, K., "A Flexible MEMs Technology and Its First Application to Shear Stress Skins," in Proc. IEEE MEMS'97 Workshop

[6] E. Torres-Jara, K. Gilpin, J. Karges, R.J. Wood and D. Rus, "Composable Flexible Small Actuators Built from Thin Shape Memory Alloy Sheets", IEEE Robotics and Automation Mag. vol. 17, no. 4, pp. 78-87, 2010

[7] Jong-Hyun Ahn, "Heterogeneous Three-Dimensional Electronics by Use of Printed Semiconductor Nanomaterials", Science 2006, V314, 1754

[8] W. Christiaens, E. Bosman, and J. Vanfleteren, "UTCP: A novel polyimide-based ultrathin chip packaging technology," IEEE Trans. Comp. Packag. Technol., vol. 33, no. 4, pp. 754–760, Dec. 2010

[9] Frederick B., "Novel Technologies for Elastic Microsystems: Development, Characterization and Applications 2011", IEICE Trans on comms, 2007, E90-B(9), 2225

[10] Dae-Hyeong K. et al,"Epidermal Electronics", Science, 12 August 2011: Vol. 333 no. 6044 pp. 838-843

[11] 3D-WLP: Ultra-Thin-Chip Stacking, www.imec.be/ScientificReport/SR2008/HTML/1224991.html, accessed Sept. 22, 2015

[12] Radhika N., "Towards a Programmable Material", MIT Artificial Intelligence Lab, 2000

[13] An Origami-Inspired Approach to Worm Robots IEEE/ASME Trans on Mechatronics, Vol. 18, No. 2, April 2013

[14] A Giant leap for Space Telescopes, https://str.llnl.gov/str/March03/Hyde.html, accessed Sept. 22, 2015.

[15] Tabata, et al: patent on Deployable Antenna "http://www.faqs.org/patents/app/20120193498", accessed Sept. 22, 2015

[16] I-Chun Cheng and Sigurd Wagner, Flexible Electronics: Materials and Applications. ISBN 978-0-387-74362-2, 2009

[17] William S. Wong and Alberto Salleo, EDS, Flexible Electronics: Materials and Applications ISBN 978-0-387-74362-2, 2009

[18] Lacour SP, Wagner S, Huang Z, Suo Z, Stretchable gold conductors on elastomeric substrates. Appl Phys Lett 82:2404–2406, 2003

[19] Stephanie P. Lacour, Harsha Prahahlad "Mechatronic System of Dielectric Elastomer Actuators Addressed by Thin Film Photoconductors on Plastic", Sensors and Actuators A: Physical, vol. 111 issue-2, Mar 2004

[20] Elisabeth Smela, "A microfabricated Movable Electrochromic "Pixel" Based on Polypyrrole", Advanced Materials, issue 11, no. 16, 1999

[21] Jamie K Paik, Elliot Hawkes, "A Novel Low-Profile Shape Memory Alloy Torsional Actuator", IOP Science, ser., pp. 9, Oct. 2010

[22] Erik D. Demaie et al, "A Universal Case Folding Pattern for Folding Orthogonal shapes", Cornell University Press, Sept. 2009

[23] Byoungkwon An, Daniela Rus, "Designing and Programming Self –Folding Sheets", Robotics and Autonomus Systems, In Press, Aug 2013

[24] Image courtesy of Distributed Robotics Laboratory at MIT, http://groups.csail.mit.edu/drl/wiki/

[25] Simon David Guest, "Deployable Structure: Concept and Analysis", PhD Dissertation, University of Cambridge, 1994

[26] Prowald, "Large Deployable Antennas - Mechanical Concepts", Keck Institute for Space Studies: Large Space Apertures Workshop, Caltech, Nov 2008

[27] Cadogan, Grahne "Deployment Control Mechanisms for Inflatable Space Structures",33rd Aerospace Mechanisms Conference, May 1999

[28] A. Jain, Robot and Multibody Dynamics: Analysis and Algorithms, ISBN 978-1-4419-72668-8

[29] Seborg, D. E., T. F. Edgar, and D. A. Mellichamp. 1989. Process Dynamics and Control, John Wiley & Sons, NY